

# On the Thrust of Self-Field MPD Thrusters <sup>\*</sup>

Edgar Choueiri<sup>†</sup>

Electric Propulsion and Plasma Dynamics Laboratory (EPPDyL)  
Princeton University

IEPC-97-121<sup>‡</sup>

## Abstract

The Maecker formula has long been used to explain the scaling of the thrust of self-field magnetoplasma-dynamic thrusters (MPDTs) with the total current. The formula is shown to be too simplistic to account for the trends in measured thrust data which exhibit departures from the model especially at low current. We show that these departures cannot simply all be attributed to electrothermal effects. Instead, we find that at high currents, the departures can be explained by the evolution of the current densities over the electrode surfaces which influence the spatial distribution of the volumetric Lorentz force densities. At low current levels the departures are attributed to the scaling of gasdynamic pressure distributions induced by the pinching components of the volumetric electromagnetic forces. The insight was used to formulate a more accurate empirically-based model for the scaling of the thrust of an MPDT.

## 1 Introduction

It is useful to have a simple analytical model or formula that can readily be used to predict the scaling of the thrust of magnetoplasma-dynamic thrusters (MPDTs) for a wide range of interesting operation parameters (e.g. current, mass flow rate, geometry, propellant type, etc.). Such a formula would be useful for characterizing thruster performance as well as for system and mission analysis. The Maecker equation, described below, is such a formula. However, as we shall see, it can suffer from substantial inaccuracies when applied to real thrusters under many conditions of interest.

The MPDT is considered to be an electromagnetic accelerator where the acceleration is primarily due to the action of the Lorentz force. In this paper we will be concerned only with the self-field MPDT<sup>1</sup> (with no applied magnetic field). The thrust produced by

a coaxial self-field electromagnetic plasma accelerator was first treated analytically by Maecker[1] and expounded by Jahn[2]. The resulting expression, often referred to as the Maecker formula, simply states that

$$T = \frac{\mu_o}{4\pi} \left( \ln \frac{r_a}{r_c} + \frac{3}{4} \right) J^2, \quad (1)$$

where  $T$  is the thrust,  $\mu_o$  is the magnetic permeability of free space,  $J$  is the total current driven between the electrodes and  $r_a$  and  $r_c$  are the anode and cathode radii. It is convenient for our discussion to define a dimensionless thrust coefficient,  $C_T$ , of order unity,

$$C_T \equiv \frac{4\pi}{\mu_o} \frac{T}{J^2} \quad (2)$$

which, for the case of the Maecker formula, is

$$C_T = \ln \frac{r_a}{r_c} + \frac{3}{4}. \quad (3)$$

Most notable in the Maecker formula is that the thrust coefficient is independent of the total current  $J$ , mass flow rate  $\dot{m}$  and type of propellant used.

Although the Maecker formula is derived from an idealized model of the MPDT, it has often been indiscriminately applied to explain the scaling of the thrust of real MPDTs. Not surprisingly, the invariance with  $J$ ,  $\dot{m}$  and propellant predicted by the formula is most often contradicted by experimental thrust measurements. This is starkly illustrated in Fig. (1) where the measured thrust coefficient of an MPDT (obtained, to a constant, by dividing the measured thrust with the square of the measured current) is plotted versus the measured current for two different argon mass flow rates along with the constant  $C_T$  of the Maecker formula.

The argon thrust measurements were made by Gilland[3] using the Princeton Benchmark Thruster (PBT) (shown schematically in Fig. (3)), however the general trends are typical of data from other thrusters. The following features and trends can be noted from that plot: 1) Generally,  $C_T$  is dependent on the mass flow rate and current unlike in the Maecker formula. 2) At high current levels, the Maecker model overpredicts  $C_T$  by more than 20%. 3) The dependence on the mass flow rate becomes more pronounced, as the current is lowered. 4) At low current levels, the measured  $C_T$  can easily reach

<sup>\*</sup>Research supported by NASA-JPL's program on advanced propulsion.

<sup>†</sup>Chief Scientist at EPPDyL. Assistant Professor, Applied Physics Group, MAE Dept. and Associated Faculty at the Dept. of Astrophysical Sciences.

<sup>‡</sup>Presented at the 25th International Electric Propulsion Conference, Cleveland Ohio, August 24-28, 1997.

<sup>1</sup>From here on, MPDT refers to the self-field version only.

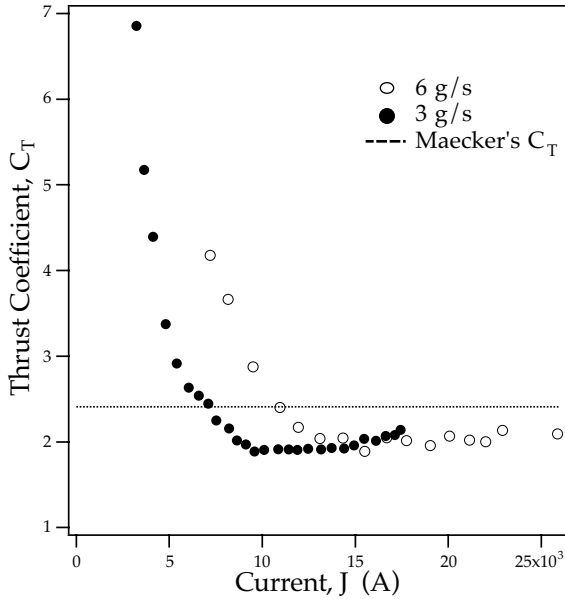


Figure 1: Comparison of the Maecker thrust coefficient with that measured[3] for the Princeton Benchmark Thruster with two different argon mass flow rates. ( $r_a/r_c = 5.26$ )

more than 250% of the Maecker value. 5) The current value at which this transition happens occurs at a lower current when the mass flow rate is decreased.

At high current levels, the discrepancy is often reconciled in the literature by substituting for the constant  $3/4$  in Eq. (1) a value that causes the model to better fit the data, or by replacing the thrust coefficient, given in Eq. (3) by  $\ln(r_a/r_c)_{eff}$  where  $(r_a/r_c)_{eff}$  is an “effective” value that provides better fit to the formula. These adjustments are often arbitrary and in both instances,  $C_T$  remains constant for a given thruster.

It is also often assumed that the departure at low current levels must be linked to an increase in the prominence of electrothermal acceleration. However, from experimental data such as those in Fig. (1), we note that at low current levels  $C_T$  scales with  $J^{-n}$  where  $n$  is between 3 and 4. This implies that the thrust (proportional to  $C_T J^2$ ) produced by this additional mechanism, must scale *inversely* with  $J$  raised to a power greater than 1. It is difficult to explain how electrothermal acceleration can be made to decrease with increasing electrical power.

**The Tikhonov formula** Before presenting a detailed analysis, it is informative to consider another simple MPDT thrust formula that has been proposed by Tikhonov[4, 5]. Unlike the Maecker formula, that of Tikhonov allows for a  $C_T$  that does vary with the current.

Tikhonov treats the case of a cylindrical MHD channel flow in the MPDT under the following assumptions: 1) Quasi-one-dimensional flow, 2) sin-

gle fluid, single temperature, 3) isothermal and 4) high magnetic Reynolds number. By setting the downstream end of the channel to be at the section where both the magnetic and thermal pressure become equal, and the upstream end to be at a section immediately behind all the enclosed current, he derives the following simple expression for  $C_T$ ,

$$C_T = \frac{\gamma + 1}{2} + \frac{\alpha_o^{-2}}{2}, \quad (4)$$

where  $\alpha_o$  is a dimensionless parameter evaluated at the upstream end of the channel,

$$\alpha_o = \frac{\gamma \mu_o J^2}{8\pi a_o \dot{m}}, \quad (5)$$

$\gamma$  is the specific heat ratio of the propellant and  $a_o$  is the ion acoustic speed evaluated at the upstream end. Notably, the expression is independent of the thruster’s  $r_a/r_c$ , the propellant ionization potential and much of the geometrical details of the electrodes. Furthermore, it states that when  $J^2/\dot{m}$  becomes high, the thrust coefficient is simply

$$C_T \simeq \frac{\gamma + 1}{2} \quad \text{when } \alpha_o \gg 1, \quad (6)$$

which for a monatomic gas has a value of 1.33.

It is obvious from Fig. (2) that this formula underpredicts  $C_T$ . It is interesting to note, however, that the Tikhonov model clearly shows the trend of increasing  $C_T$  with decreasing current and specifically a scaling of  $J^{-4}$  for the thrust coefficient as the current is decreased.

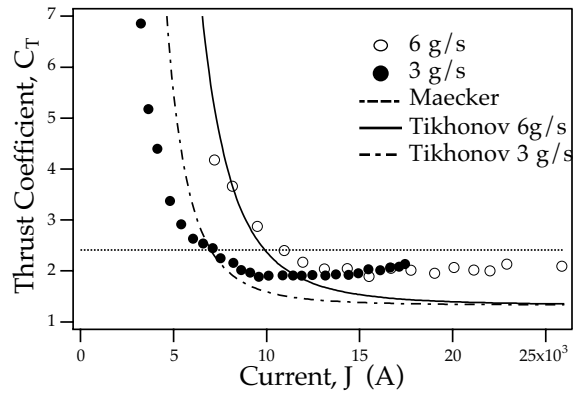


Figure 2: Comparison of the Tikhonov thrust coefficient with the measured thrust coefficient of the PBT plotted versus the measured current for two different argon mass flow rates. Also shown is the constant Maecker  $C_T$ . (The ion acoustic speed was calculated for a temperature of 1 eV)

Using the results of theoretical and experimental research carried at EPPDyL over the span of two decades, we explore the scaling and dependencies of the thrust and its departure from the simple prescriptions described above. The insight is then used to formulate a more accurate empirically-based model for the scaling of the thrust of the PBT.

## 2 Detailed Analysis of the Thrust of an MPDT

**First-principles model.** It was Rudolph[6] who analytically treated the thrust of the Princeton benchmark thruster (PBT) starting from first principles. At the time of that work in 1980, there were no direct thrust measurements available on the PBT. The extensive database available now, will allow us to confirm the predicted trends and better understand the differences between measured thrust and the predictions of the simpler models. We will follow the analysis in ref. [6] and include some effects neglected in that work. These additional effects are essential to explain the departures of the data from the simple models such as the Maecker formula.

Figure 3 shows a schematic of the PBT configuration with a central cathode (10 cm long), and an outer anode (5.1 cm inner radius). The neutral gas is injected from ports in the backplate (left side of that figure), which like the chamber walls, is an insulator. Also shown in the figure are the cylindrical coordinate system and the boundary (dashed line) of the control volume adopted for the analysis.

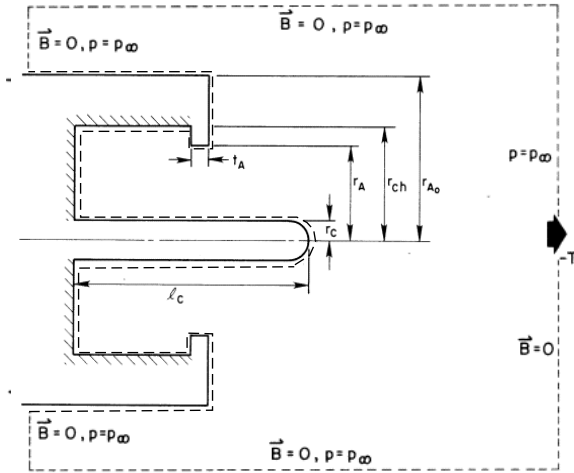


Figure 3: Control volume used in deriving a thrust equation for the Princeton benchmark thruster[6]. The dashed line represents the boundary of the control volume used in the thrust analysis. For the particular thruster used in the thrust experiments we have  $r_c = .95$  cm,  $r_a = 5.1$  cm,  $r_{ao} = 9.3$  cm,  $r_{ch} = 6.4$  cm,  $t_a = .95$  cm and  $l_c = 10$  cm.

The control volume denotes the region where electromagnetic, gasdynamic and viscous shear forces act on the propellant thus producing a momentum flux. The thrust is equal to the net momentum flux carried away by the propellant flow. The control volume is chosen such that all of its free boundaries are far enough from the thruster as to warrant setting the magnetic field there to zero and the pressure equal to the ambient pressure. With these boundary conditions, the only forces that need to be considered are

those on the thrust surfaces and inside the control volume. Since we are interested in thrust as the axial component of the force, we can write

$$\int_S \rho u_z (\mathbf{u} \cdot d\mathbf{S}) = + \int_V j_r B_\theta dV - \int_S p (\mathbf{z} \cdot d\mathbf{S}), \quad (7)$$

where  $S$  and  $V$  are the surface and volume of the control volume,  $\mathbf{z}$  is the unit vector and the rest of the symbols have their usual meaning. The left side of the above equation is the net momentum flux which is the difference between the thrust and the “cold” thrust  $T_c$  due to the cold slow gas entering the control volume. We therefore have,

$$T = T_c + \int_V j_r B_\theta dV - \int_S p (\mathbf{z} \cdot d\mathbf{S}), \quad (8)$$

The second term on the right hand side represents the contribution of  $j_r B_\theta$ , the axial component of the Lorentz force density, which acts to “blow” the plasma out. This term will be referred to as  $T_b$ , the “blowing” contribution to thrust. The radial component of the Lorentz force density,  $j_z B_\theta$  acts to pinch the plasma and contributes to axial thrust through the unbalanced effect of the gasdynamic pressure on some surfaces of the accelerator. Consequently the second integral on the right hand side is an integral of the gasdynamic pressure and represents the “pinching” contribution of the Lorentz force to the axial thrust and is termed  $T_p$ . This integral contains, implicitly, the effects of  $j_z B_\theta$ .

The cold gas contribution  $T_c$  is typically much smaller than the total thrust and will be neglected in this analysis. Also neglected in the above equation are viscous effects. In SI units, a typical plasma viscosity of  $10^{-5}$ , a velocity of  $10^4$  and a boundary layer thickness of about 1 mm yield a viscous force of  $10^{-2}$  N/cm<sup>2</sup>[7]. For a thruster whose total wall surface area is on the order of 100 cm<sup>2</sup>, the viscous force is negligible compared to the thrust of the PBT which is typically on the order of 100 Newtons.

**Blowing Contributions.** The evaluation of  $T_b$  through volume integration, as prescribed by the second term on the right hand side of Eq. (8), requires a knowledge of the details of the current distribution inside the chamber. However, by using the concept of the magnetic stress tensor, the volume integral can be replaced by a far more useful surface integral[2, 6]. By definition, the Maxwell stress tensor,  $\tilde{\beta}$ , satisfies the following equation,

$$\nabla \cdot \tilde{\beta} = \mathbf{j} \times \mathbf{B} + \frac{\mathbf{B}(\nabla \cdot \mathbf{B})}{\mu_0}, \quad (9)$$

which when combined with Maxwell’s equations for the divergence and curl of the magnetic field, yields

$$\nabla \cdot \tilde{\beta} = \frac{(\nabla \times \mathbf{B}) \times \mathbf{B}}{\mu_0}. \quad (10)$$

This equation allows us to relate the volume integral of the Lorentz body force density to a surface integral

through the divergence theorem:

$$T_b = \int_V j_r B_\theta dV = \int_V (\nabla \cdot \tilde{\beta})_z dV = \int_S (\tilde{\beta} \cdot d\mathbf{S})_z. \quad (11)$$

For a coaxial self-field MPDT with a symmetric discharge, the magnetic field has only an azimuthal component and the magnetic stress tensor takes the form

$$\tilde{\beta} = \frac{1}{\mu_o} \begin{bmatrix} -\frac{B_\theta^2}{2} & 0 & 0 \\ 0 & -\frac{B_\theta^2}{2r^2} & 0 \\ 0 & 0 & -\frac{B_\theta^2}{2} \end{bmatrix}. \quad (12)$$

The only areas of the control volume surface shown in Fig. (3) that contribute to the surface integral in Eq. (11) are the four that are perpendicular to the thrust axis and over which the magnetic field is finite. These are the backplate, the anode front (downstream) surface, the anode back (upstream) surface and the tip of the cathode. The anode lip, which in reality is rounded, will be approximated by a flat surface as shown in Fig. (3) where all the physical dimensions of the PBT that are needed for the evaluation of the integral are defined.

The resulting contributions of the four surfaces to  $T_b$  are quoted below. Details of the integration can be found in ref. [6].

#### Backplate blowing contribution:

$$[T_b]_{BP} = \frac{\mu_o}{4\pi} \ln \frac{r_{ch}}{r_c}. \quad (13)$$

**Anode inner face blowing contribution:** Assuming a uniform current density,  $j_i$ , on the inner face of the anode, this contribution is:

$$\begin{aligned} [T_b]_{AIF} &= -\frac{\mu_o}{4\pi} \left[ (J^2 - 2\pi r_{ch}^2 j_i J + \pi^2 r_{ch}^4 j_i^2) \ln \frac{r_{ch}}{r_a} \right. \\ &+ (\pi J j_i - \pi^2 r_{ch}^2 j_i^2) (r_{ch}^2 - r_a^2) \\ &+ \left. \frac{\pi^2 j_i^2}{4} (r_{ch}^4 - r_a^4) \right]. \end{aligned} \quad (14)$$

#### Anode outer face blowing contribution:

$$\begin{aligned} [T_b]_{AOF} &= \frac{\mu_o}{4\pi} \left[ \pi^2 r_{ao}^4 j_o^2 \ln \frac{r_{ao}}{r_a} \right. \\ &- \pi^2 r_{ao}^2 j_o^2 (r_{ao}^2 - r_a^2) \\ &+ \left. \frac{\pi^2 j_o^2}{4} (r_{ao}^4 - r_a^4) \right] \end{aligned} \quad (15)$$

where  $j_o$  is the current density on the outer face of the anode.

#### Cathode tip blowing contribution:

$$[T_b]_{CT} = \frac{\mu_o \phi^2 J^2}{4\pi} \left[ \frac{3}{2} - 2 \ln 2 \right]. \quad (16)$$

where  $\phi$  is the fraction of the total current attached at the hemispherical tip of the cathode.

The final expression for  $T_b$  is obtained by summing all four contributions given by Eqs. (13), (14), (15) and (16).

**Pinching Contributions** In order to evaluate the surface integral of the gasdynamic pressure in Eq. (8), we consider the radial momentum balance:

$$\rho u_r \frac{\partial u_r}{\partial r} = -\frac{\partial p}{\partial r} - j_z B_\theta \quad (17)$$

where the term  $\rho u_z \partial u_r / \partial z$  does not appear because  $u_z$  is zero on the solid surfaces over which the integral will be evaluated (backplate, inner and outer anode faces and the cathode tip). This yields the following expression for  $p(r, z)$  along the surfaces of the control volume,

$$p(r, z) = \int_r^{r_o} \rho u_r \frac{\partial u_r}{\partial r} dr + \int_r^{r_o} \frac{B_\theta}{\mu_o r} \frac{\partial r B_\theta}{\partial r} dr + p(r_o, z) \quad (18)$$

where Maxwell's  $\nabla \times \mathbf{B}$  equation was used to eliminate  $j_z$ . The last term,  $p(r_o, z)$ , is the integration constant taken as the gasdynamic pressure at an arbitrary radius  $r_o$ .

The magnitude of the integrand in the first integral can be estimated to be on the order of  $10^4 \text{N/m}^3$  using an upper limit on the plasma density ( $10^{22} \text{m}^{-3}$  (which gives  $\rho = 6.6 \times 10^{-4} \text{kg/m}^3$  for argon), velocities of  $10^4 \text{m/s}$  and a characteristic length of 5 cm. This magnitude is typically quite lower than that of the radial pinching force density as estimated from measurements by Rudolph[6]. Consequently Rudolph assumes the radial flow term to be negligible in his analysis. We shall see that in order to explain the rise in  $C_T$  at lower currents the radial flow term should not be neglected at least for the case of the backplate pinching contribution to thrust.

**Backplate pinching contribution.** The pinching contribution of the backplate part of the control volume presents an interesting singularity as the second integral in Eq. (18) vanishes because all the current is downstream of that boundary and that  $r B_\theta$  is a constant there. This implies that the pressure gradient on that surface is balanced by the radial flow term only. This gives a thrust contribution of

$$\begin{aligned} [T_p]_{BP} &= \left[ -\int_S p(\mathbf{z} \cdot d\mathbf{S}) \right]_{BP} \\ &= p(r_{ch}, z_o) \pi (r_{ch}^2 - r_c^2) \\ &+ \int_{r_c}^{r_{ch}} 2\pi r \left[ \int_r^{r_{ch}} \rho u_r \frac{\partial u_r}{\partial r} dr \right] dr, \end{aligned} \quad (19)$$

where  $z_o$  refers to the axial position of the backplate. The pressure  $p(r_{ch}, z_o)$  was measured at the backplate by Cory[7] and we will use his measurements in the calculations below. We lack, however, an experimental characterization that would allow us to estimate the radial flow term in the above equation. If this

flow term is neglected, as was done by Rudolph[6], the pressure profile is flat and the thrust contribution is a constant given by  $p(r_{ch}, z_o)\pi(r_{ch}^2 - r_c^2)$ . A finite (non-uniform) radial velocity profile, on the other hand, would induce a pressure radial profile at that surface that is peaked at the cathode. Consequently, a better approximation than a flat profile would be a parabolic one centered at the cathode and modeled as

$$p(r, z_o) = b - ar^2, \quad (20)$$

where

$$a = \frac{p(r_c) - p(r_{ch})}{r_{ch}^2 - r_c^2}; \quad b = p(r_c) + \frac{p(r_c) - p(r_{ch})}{r_{ch}^2 - r_c^2} r_c^2, \quad (21)$$

and where, for the case of the backplate, the pressures are those at  $z = z_o$ . After integration, this yields the following thrust contribution

$$[T_p]_{BP} = b\pi(r_{ch}^2 - r_c^2) - \frac{a\pi}{2}(r_{ch}^4 - r_c^4). \quad (22)$$

While the measurements of Cory[7] will be used for  $p(r_{ch}, z_o)$ , the unknown term  $p(r_c, z_o)$  becomes the only free parameter of the model. The value for  $p(r_c, z_o)$  will be inferred from the thrust data as will be shown further below. Rudolph's approximation of neglecting the radial flow term is equivalent to setting  $p(r_c, z_o)$  equal to  $p(r_{ch}, z_o)$ . This would lead to an underestimate of the pinching contribution to thrust and cannot account for the rise of  $C_T$  with decreasing current as will be shown in the evaluation at the end of this section.

**Anode inner face pinching contribution.** Downstream of the backplate end of the control volume, the second integral in Eq. (18) quickly dominates over the radial flow term and consequently, the pressure profile may be assumed to be induced mainly by the Lorentz term. Using the same assumptions as for the blowing contribution in Eq. (14), the integration yields[6]:

$$\begin{aligned} [T_p]_{AIF} &= \frac{\mu_o}{4\pi} [(j_i^2 \pi^2 r_{ch}^4 + j_i^2 \pi^2 r_{ch}^2 r_a^2 \\ &- 2Jj_i \pi r_{ch}^2) \frac{r_{ch}^2 - r_a^2}{2r_{ch}^2} \\ &- (2r_a^2 j_i^2 \pi^2 r_{ch}^2 - 2Jj_i \pi r_a^2) \ln \frac{r_a}{r_c}] \\ &- \pi(r_{ch}^2 - r_a^2) p(r_{ch}, z_o). \end{aligned} \quad (23)$$

Where we have assumed again the pressure constant to be  $p(r_{ch}, z_o)$ .

**Anode outer face pinching contribution.** The plasma density on the 200 cm<sup>2</sup> anode of the PBT does not exceed an upper bound of 10<sup>20</sup> m<sup>-3</sup>[7] so that even for a temperature as high as 5 eV, the pressure force will be less than 2N and can be neglected.

**Cathode tip pinching contribution.** This contribution is also quite small because typically  $\phi$  is on the order of 10%. Following the prescriptions used above to get the blowing contribution at the cathode tip, and neglecting the radial flow term, the integration of Eq. (20) yields[6]:

$$[T_p]_{CT} = \frac{\mu_o}{4\pi} \frac{\phi^2 J^2}{12} + p(r_c, z_{tip}) \pi r_c^2, \quad (24)$$

where  $p(r_c, z_{tip})$  is the pressure at the cathode tip available from experiments.

The total thrust is the total sum of the blowing contribution expressed in Eqs. (13), (14), (15), (16) and the pinching contributions expressed in Eqs. (22), (23) and (24).

**Comparison to the Maecker formula.** The Maecker formula as derived and discussed by Jahn[2] can be obtained by applying the Maxwell stress tensor approach to a simple cylindrical control volume (shown in Fig. 8-19 of ref. [2]). This choice of control volume is equivalent to considering the thruster as an infinite cylinder without a backplate.

The differences between the resulting simple formula and the detailed model derived above can be attributed to the following: 1) The Maecker formula does not include the effects of current attachment on surfaces that are not parallel to the thruster axis. 2) While the Maecker formula assumes that all the current attaches uniformly at the cathode tip, the treatment above allows for a more diffusive current attachment over the cathode length with a fraction  $\phi J$  attaching at the tip. 3) In the Maecker formula, the blowing component contributes a term of  $(\ln r_a/r_c + 1/4)$  to  $C_T$  assuming a uniform current density on the cathode surface, and a constant of 1/2 from the pinching pressure on the cathode tip giving a constant equal to 3/4. It does not include the effects of pinching pressure on the backplate of the thruster.

For the PBT at high currents, the blowing contribution at the backplate, dominates while the terms for blowing and pinching at the cathode tip, even if  $\phi$  is near unity, contribute a thrust coefficient below .2, which is far lower than the corresponding 3/4 term in the Maecker formula. We shall see below that at high currents, the pinching contribution at the backplate is not high enough to exceed the  $C_T$  of the Maecker formula. At low currents, however, the pinching pressure effects on the backplate cause an enhancement in  $C_T$  above the Maecker value.

**Semi-empirical evaluation.** So far the thrust model, represented by Eqs. (13), (14), (15), (16), (22), (23) is purely analytical from first principles. However, it cannot inform us on how  $C_T$  varies with the current since we lack a prescription of how the parameters

$$j_i, j_o, \phi, P(r_c, z_{tip}) \text{ and } p(r_{ch}, z_o), \quad (25)$$

vary with the total current  $J$ . A prescription of this sort can be obtained from experimental measurements of current distribution along the electrodes as a function of  $J$  and pressure measurements. The use of an experimental prescription of these parameters will render the model semi-empirical and applicable only for the conditions (e.g.  $\dot{m}$ , propellant type) under which the thruster, used for the experiments, was operated. Such a semi-empirical evaluation of the model is useful in showing the general thrust scaling trends and will be of guidance to our efforts to formulate a more generalized thrust scaling relation in section 3.

Using the current density measurements reported in Refs. [6, 9, 10], the evolution of  $j_i$  and  $j_o$  (along the anode inner and outer faces) with the total current  $J$  was deduced to have the following general trend. Below a first transition current  $J_{t1}$ , the current attaches entirely on the inner face of the anode. Above  $J_{t1}$ , but below another transition current  $J_{t2}$ ,  $j_i$  on the inner face stays constant while  $j_{lip}$  on the anode lip becomes finite and increases with increasing  $J$  until  $J_{t2}$  is reached. Above this limit, any additional increase in  $J$  is attached at the outside face of the anode while both  $j_i$  and  $j_{lip}$  stay constant. By requiring that  $J = j_i S_i + j_{lip} S_{lip} + j_o S_o$  (where  $S$  is the area of each surface) and assuming the current densities to be uniform over these areas, we can write:

$$\begin{aligned}
J \leq J_{t1} : j_i &= \frac{J}{S_i}; j_{lip} = 0; j_o = 0 \\
J_{t1} \leq J \leq J_{t2} : j_i &= \frac{J_{t1}}{S_i}; j_{lip} = \frac{J - J_{t1}}{S_{lip}}; j_o = 0 \\
J_{t2} < J : j_i &= \frac{J_{t1}}{S_i}; j_{lip} = \frac{J_{t2} - J_{t1}}{S_{lip}}; \\
j_o &= \frac{J - J_{t2}}{S_o}. \quad (26)
\end{aligned}$$

For the PBT operating with 6 g/s of argon, we can deduce from ref. [6],  $J_{t1} = 3.7$  kA and  $J_{t2} = 14$  kA.

The dependence of  $p(r_{ch}, z_o)$  on the current was measured by Cory[7] and is given by

$$p(r_{ch}, z_o) = 6.5 \times 10^{-4} J^{1.5} \text{ N/m}^2 \quad (27)$$

for 6 g/s of argon. Finally, from current density measurements and momentum balance considerations[6] we have:

$$p(r_c, z_{tip}) = .263J \text{ N/m}^2, \quad (28)$$

and  $\phi$  is essentially constant at .2.

With these empirical specifications all the components of thrust can be calculated with the exception of  $[T_p]_{BP}$  which requires knowledge of the dependence of  $p(r_c, z_o)$  on  $J$ . Consequently, we calculated all the other components of thrust and subtracted their sum from the measured (total) thrust data at 6 g/s. The remaining contribution represents the pinching contribution at the backplate end of the control volume. Figure 4 shows the evolution of  $p(r_c, z_o)$  vs  $J$  that is required for Eq. (2) to fit the backplate pinching contribution inferred from the data. It can be noted

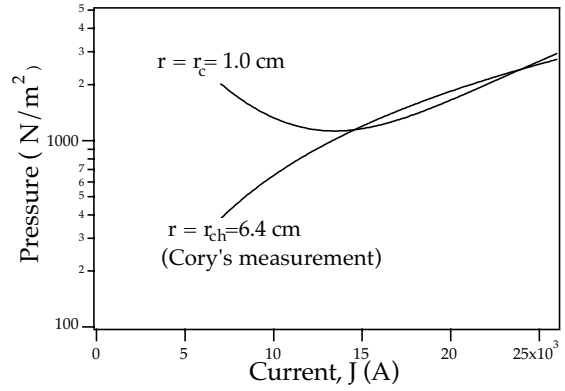


Figure 4: Evolution of the gasdynamic pressure on the backplate at the cathode ( $r = r_c$ ) inferred from the measured data. Also shown is the pressure at a radius ( $r = r_{ch}$ ) as measured by Cory[7] (cf. empirical formula in Eq. (27))

that as the current is increased beyond about 14 kA, the pressure on that boundary at the cathode radius becomes essentially equal to the pressure at a radius  $r_{ch}$  and is given by Cory's empirical formula. This means that, above this current, the pressure radial profile is flat as assumed by Rudolph[6]. However, below that current level, a substantial difference between the pressure at  $r_c$  and that at  $r_{ch}$  is required to explain the data. The pressure radial profiles corresponding to the curves in Fig. (4) are shown in Fig. (5) for four different current levels.

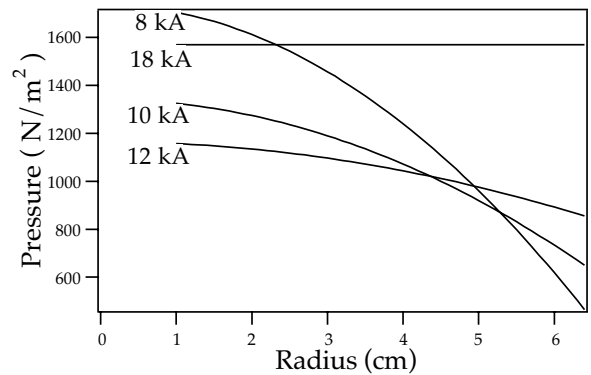


Figure 5: Radial profiles of the pressure at the backplate corresponding to the curves shown in Fig. (4), for four different current levels.

Figure 6 shows the contributions of the various blowing and pinching components to  $C_T$  along with their total sum. It is clear from this figure that at high current levels, the main contribution to the thrust is from the blowing component at the backplate with a small contribution from the pinching component which, from Fig. (4), can be seen to be fully accounted for by Cory's pressure measurements at  $r = r_{ch}$ . As the current is decreased, the pressure

at the cathode end of the backplate must increase above its value at higher radii in order to account for the rise in  $C_T$ .

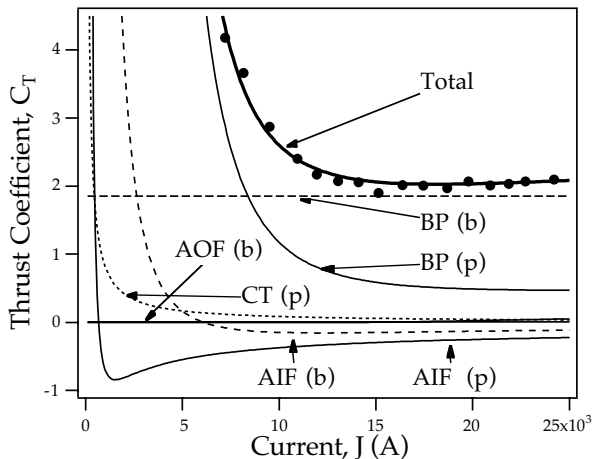


Figure 6: Contributions of the various blowing and pinching components to  $C_T$  along with their total sum for the PBT operated with 6 g/s of argon. Also shown are the measured data.

The rise in  $C_T$  at lower current, according to this picture, should not be termed an “electrothermal” effect as it is not simply due to an expansion of an ohmically heated gas but the result of the evolution of gasdynamic pressure distributions induced by the pinching effect of the volumetric Lorentz force densities.

### 3 Generalization to a Simple Scaling Relation

We now use the insight gained so far to formulate a simple scaling relation that embodies the effects described above and that would also be valid for other mass flow rates and propellants (than 6 g/s of argon).

**The critical ionization velocity and the dimensionless current  $\xi$ .** Numerous experiments (see the citations in ref. [8]) on the MPDT have shown that the following dimensionless parameter

$$\xi = J / \left[ \frac{\dot{m}^{1/2} (2\epsilon_i/m_i)^{1/4}}{\left( \frac{\mu_o}{4\pi} \ln \frac{r_a}{r_c} \right)^{1/2}} \right] \quad (29)$$

(where  $m_a$  and  $\epsilon_i$  are the mass and the first ionization potential of the neutral atom) scales various aspects of MPDT behavior. The first scaling relations for MPDT characteristics (voltage and thrust) based on this parameter were derived in 1987[11].

A physical interpretation for the scaling with  $\xi$  can be made as follows. In the MPDT, ionization is a sig-

nificant energy sink whose scaling, under nominal operation of the thruster, is strongly tied to the magnitude of the energy in the acceleration (useful) “sink”. The strong tie between these two sinks is suspected to be related to the role of plasma instabilities in controlling and enhancing ionization. (Evidence on the role of plasma instabilities in MPDT ionization was presented in ref. [12].) Since instabilities in MPDTs are of the current-driven type[13], and since acceleration in the MPDT is also current-driven, both sinks are sharing the same source, namely the current. A nominal regime for MPDT operation can thus be defined in terms of this “equipartition” of energy (or power) sinks which can be stated, in terms of power, as

$$\frac{1}{2} T u_{ex} = \dot{m} \frac{\epsilon_i}{M}, \quad (30)$$

which by definition, only holds near the nominal operation point. The velocity  $u_{ex}$  in this expression is that of the plasma exhaust. Since  $T = (\mu_o/4\pi) C_T J^2$ , the above relation gives

$$\frac{\mu_o}{4\pi} C_T J^2 u_{ex} = \dot{m} u_{ci}^2, \quad (31)$$

where  $u_{ci}$  is defined as

$$u_{ci} \equiv \left( \frac{2\epsilon_i}{m_a} \right)^{1/2}, \quad (32)$$

and is generally known as the critical ionization velocity. For xenon, argon and lithium,  $u_{ci}$  is 4.22, 8.72 and 12.24 km/s respectively.

We define “nominal operation” to be that for a thruster current that produces an exhaust velocity equal to the critical ionization velocity. That current is termed the critical ionization current,  $J_{ci}$ . From the above equation we have,

$$J_{ci} = \left( \frac{\dot{m} u_{ci}}{\frac{\mu_o}{4\pi} C_T} \right)^{1/2}. \quad (33)$$

This characteristic current is used to nondimensionalize the thruster current giving us the dimensionless parameter  $\xi$  defined as

$$\xi \equiv \frac{J}{J_{ci}}, \quad (34)$$

which is written more explicitly in Eq. (29) where the thrust coefficient  $C_T$  was taken, to a first order, to be  $\ln \frac{r_a}{r_c}$ . (For  $\xi$  near 1, a better approximation for  $C_T$ , as will be seen later, is  $\ln \left( \frac{r_a}{r_c} + 1 \right)$ ).

The parameter  $\xi$  can be thought of as a similarity parameter in the sense that two thrusters operating at the same value of  $\xi$  are expected to exhibit some similar characteristics. Since this similarity is borne out by numerous experiments, we shall adopt it axiomatically in our formulation of a thrust scaling relation and verify its applicability by testing the resulting scaling formula with experimental data over a wide range of parameters.

**Formulation of a thrust scaling relation** From thrust data, the results of the analysis in section 2 and from the Tikhonov formula, we expect  $C_T$  at low current levels to scale with  $J^{-n}$  where  $n$  is about 4. Therefore for small values of  $\xi$ , we expect the following scaling

$$C_T \sim \xi^{-4} \quad (\text{for } \xi < 1). \quad (35)$$

At high current levels ( $\xi > 1$ ), we know from the above discussions that  $C_T$  scales weakly with the current but is not constant as in the Maecker formula. This is due to both the dominance of the back-plate blowing contribution and the finiteness of all the other terms which provide the dependence on the current. This dependence is too complex to model as it relates to how the current densities distribute over the electrodes and how that distribution evolves with changing current. It would be much more useful to have a less entangled, albeit empirical, characterization of the scaling of this effect. Fortunately such a study does exist in the form of an experimental investigation carried by Kaplan[10] who found that the scaling the thrust coefficient at high current levels is such that  $e^{C_T}$  vs  $J^2/\dot{m}$  can be represented by a line whose intercept is very close to the physical value of  $r_a/r_c$ .

Based on these considerations and the fact that  $J^2/\dot{m}$  scales as  $\xi^2$  we expect the following scaling for the thrust coefficient at high values of  $\xi$ ,

$$C_T \sim \ln\left(\frac{r_a}{r_c} + \xi^2\right) \quad (\text{for } \xi > 1). \quad (36)$$

In light of all of the above we can formulate a scaling model that is a combination of Eqs. (35) and (36) in the form of

$$C_T = \frac{\nu}{\xi^4} + \ln\left(\frac{r_a}{r_c} + \xi^2\right), \quad (37)$$

where  $\nu$  is a dimensionless mass flow rate that corrects for mass flow rate effects:

$$\nu \equiv \frac{\dot{m}}{\dot{m}^*}, \quad (38)$$

and where  $\dot{m}^*$  is a reference mass flow rate presumed to be a constant and is obtained empirically from the data. Using the expression

$$C_T = \frac{\dot{m}/\dot{m}^*}{\xi^4} + \ln\left(\frac{r_a}{r_c} + \xi^2\right), \quad (39)$$

with the 6 g/s argon data, yielded

$$\dot{m}^* = 66 \text{ g/s}. \quad (40)$$

In the narrow sense of applying to data at three mass flow rates of both argon and xenon as well as for two similar thrusters with different length scales, this value for  $\dot{m}^*$  is “universal” as shown by the comparison of the model to these data.

The plots in Fig. (7) show a comparison of the model to argon and xenon thrust measurements at

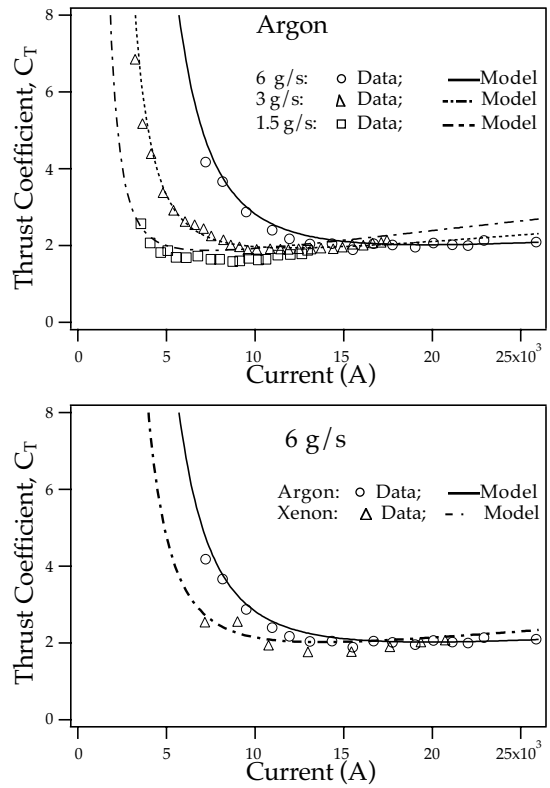


Figure 7: Comparison of the scaling formula in Eq. (39) with argon and xenon thrust measurements for various mass flow rates.

various mass flow rates (the xenon data were obtained recently at EPPDyL by Ziemer) showing that the trends in the data are well accounted for. The agreement was far worse for attempts to model hydrogen data. This could be partly related to the fact that the critical ionization velocity of hydrogen is both very high and ill-defined (diatomic molecule).

## REFERENCES

- [1] H. Maecker. *Z. Phys.*, 141(1):198–216, 1955.
- [2] R.G. Jahn. *Physics of Electric Propulsion*. McGraw-Hill, New York, 1968.
- [3] J.H. Gilland. Master’s thesis, Princeton University, 1988.
- [4] V.B. Tikhonov, et. al. IEPC-93-076.
- [5] N.V. Belan, et. al. *Stationary Plasma Thrusters (in Russian)*. KHAI, Kharkov, pp. 985, 1989.
- [6] L.K. Rudolph. PhD thesis, Princeton University, 1981.
- [7] J.S. Cory. PhD thesis, Princeton University, 1971.
- [8] E. Choueiri. *3<sup>rd</sup> International Symposium on Space Propulsion*, Beijing, China, 1997. paper-24.
- [9] A.J. Saber. PhD thesis, Princeton University, 1974.
- [10] D.I. Kaplan. Master’s thesis, Princeton University, 1982.
- [11] E.Y. Choueiri, et. al. AIAA-87-1067.
- [12] E.Y. Choueiri and H. Okuda. IEPC-93-067.
- [13] E.Y. Choueiri, et. al. IEPC-91-100.



## References

- [1] H. Maecker. Plasma jets in arcs in a process of self-induced magnetic compression. *Z. Phys.*, 141(1):198–216, 1955.
- [2] R.G. Jahn. *Physics of Electric Propulsion*. McGraw-Hill, New York, 1968.
- [3] J.H. Gilland. The effect of geometrical scale upon MPD thruster behavior. Master’s thesis, Princeton University, Princeton, NJ, USA, 1988.
- [4] V.B. Tikhonov, S.A. Semenihih, V.A. Alexandrov, G.A. Dyakonov, and G.A. Popov. Research of plasma acceleration processes in self-field and applied magnetic field thrusters. In *23<sup>rd</sup> International Electric Propulsion Conference*, Seattle, WA, USA, 1993. IEPC-93-076.
- [5] N.V. Belan, V. Kim, A.I. Oranstky, and V.B. Tikhonov. *Stationary Plasma Thrusters (in Russian)*. KHAI, Kharkov, pp. 985, 1989.
- [6] L.K. Rudolph. *The MPD Thruster Onset Current Performance Limitation*. PhD thesis, Princeton University, Princeton, NJ, USA, 1981.
- [7] J.S. Cory. *Mass, Momentum and Energy Flow from an MPD Accelerator*. PhD thesis, Princeton University, Princeton, NJ, USA, 1971.
- [8] E. Choueiri. The scaling of thrust in self-field MPD thrusters. In *3<sup>rd</sup> International Symposium on Space Propulsion*, Beijing, China, 1997. paper-24.
- [9] A.J. Saber. *Anode Power in a Quasi-Steady MPD Thruster*. PhD thesis, Princeton University, Princeton, NJ, USA, 1974.
- [10] D.I. Kaplan. Performance characteristics of geometrically scaled MPD thrusters. Master’s thesis, Princeton University, Princeton, NJ, USA, 1982.
- [11] E.Y. Choueiri, A.J. Kelly, and R.G. Jahn. MPD thruster instability studies. In *19<sup>th</sup> International Electric Propulsion Conference*, Colorado Springs, CO, USA, 1987. AIAA-87-1067.
- [12] E.Y. Choueiri and H. Okuda. Anomalous ionization in the MPD thruster. In *23<sup>rd</sup> International Electric Propulsion Conference*, Seattle, WA, USA, 1993. IEPC-93-067.
- [13] E.Y. Choueiri, A. J. Kelly, and R. G. Jahn. Current-driven plasma acceleration versus current-driven energy dissipation part II : Electromagnetic wave stability theory and experiments. In *22<sup>nd</sup> International Electric Propulsion Conference*, Viareggio, Italy, 1991. IEPC-91-100.